RSC Advances

ROYAL SOCIETY OF CHEMISTRY

www.rsc.org/advances

Journal Name

ARTICLE

Texture orientation of silver thin films grown via gas-timing radio frequency magnetron sputtering and their SERS activity

Received 00th January 20xx,
Accepted 00th January 20xx

DOI: 10.1039/x0xx00000x

www.rsc.org/

Pongbordin Ukahapunyakul[ab], Nurak Gridsadanurak[ab*], Chaweewan Sapcharoenkun[c], Alongkot Treetong[c], Panita Kasamechonchung[c], Pongtanawat Khemthong[c], Mati Horprathum[d], Supanit Porntheeraphat[d], Winadda Wongwiriyapan[e], Jiti Nukeaw[e] and Annop Klamchuen[c*]

Here we demonstrate a special technique to control a texture orientation of silver (Ag) thin films via using gas-timing (GT) rf magnetron sputtering. By utilizing GT technique, a dense structure and a high ratio of (111)/(200) of Ag films could be obtained without any applying additional energy sources. We found that the GT technique not only provides the ability to adjust the number of sputter species from the target, but also generates the self-energy assisted deposition which related to the atomic peening effect. Furthermore, we found that high (111)/(200) ratio of Ag films strongly affects on the SERS activity of Ag films due to hot spot effect. Our results highlight that the texture engineering of metal thin films could be accomplished by using GT technique.

Introduction

Texture and surface engineering of silver (Ag) thin films fabricated by sputtering technique are very attractive for several advanced technologies such as heat reflecting system for automotive glazing,[1] reduction of run-in wear of solid lubricant coatings,[2] reduction of the friction coefficient of alumina disks,[3] application in ultra large scale integrated (ULSI) circuit[4] and application for surface enhanced Raman scattering (SERS) substrate.[5-9] It has been known that the strong (111) preferred orientation of sputtered Ag films is strongly required for the electromigration resistance in electronic devices under high current densities.[10-17] Since sputtered deposited face-centered-cubic (FCC) materials, i.e. Ag, Cu and Al, correspond to the most densely packed planes in each lattice which relates to the lowest energy surface,[10-17] it is thermodynamically favorable to orient all of the grains in the film texture such that their surface normal is perpendicular to the highest density planes.[15] Therefore, the enhanced (111) preferred orientation could be promoted by increasing total energy input during thin film deposition.[14] Although several research groups have demonstrated the controllability in the texture and surface morphology of sputtered Ag thin films, the external energy sources such as substrate bias voltage,[10,14-16] heating the substrate during growth[5,11] or post annealing[5,12] and ionized magnetron sputter deposition (IMSD)[14] are necessary to include. Such external added techniques make a complex and high cost operation and are not available to fabricate sputtered Ag film at room temperature. Recently, Jiti et al. established special techniques that are available to adjust chemical composition and obtain high quality crystalline in thin films by controlling the on-off flow sequence of sputtering gas so called gas-timing (GT) and reactive gas-timing (RGT) techniques.[18-25] Another major advantage of these techniques is the change in structure coupled with high quality crystalline thin film which could be achieved at room temperature and without applying any external energy source.[18-25] Here we demonstrate the texture engineering of sputtered Ag thin films through GT rf magnetron sputtering. The dependence of RF power, working pressure and on-off gas sequence on the peak intensity of (111)/(200) ratio was investigated. We found that the GT technique as to the on-off sequence switching can be attributed to the alternate sequence between deposition mode and energy-assisted mode. Furthermore, we exhibit the utilizing of Ag thin film grown via GT technique for the SERS substrates. Our results highlight that the GT technique allows us to control and design the texture engineering of metal thin films, which can be applied in various research fields.

[a] Department of Chemical Engineering, Faculty of Engineering, Thammasat University, Pathumthani, Thailand.
[b] Center of Excellence in Environmental Catalysis and Adsorption, Thammasat University, Pathumthani 12120, Thailand.
[c] National Nanotechnology Center (NANOTEC), NSTDA, Thailand Science Park, PathumThani, Thailand
[d] National Electronics and Computer Technology Center (NECTEC), NSTDA, Pathum Thani, Thailand
[e] College of Nanotechnology, King Mongkut's Institute of Technology Ladkrabang, Chalongkrung Rd., Ladkrabang, Bangkok 10520, Thailand.

†Electronic Supplementary Information (ESI) available: Fig, S1 sbow Dependence peak intensity of (111)/(200) ratio on the resistivity of Ag thin films. Fig. S2 show S2. The difference in the deposition rate between turn-on and turn-off gas (ΔR).
See DOI: 10.1039/x0xx00000x

Experimental

Fabrication of silver thin film

Ag thin films were fabricated on silicon (Si) (111) by using GT rf reactive magnetron sputtering technique.[18-25] A 3-inch diameter with a 0.25-inch thick of silver target (99.99%, Kurt J. Lesker Company) was used as a sputtering target. The Si (111) substrates were cleaned by an alcohol process, which Si (111) substrates were ultrasonically cleaned with acetone, ethyl alcohol and deionized water for 10 min, respectively, and then dried with the nitrogen flow. The samples were then transferred to the high vacuum chamber for thin film deposition. Distance between target-to-substrate was set at 70 mm. The substrates were mounted on a rotational holder substrate, which was driven by a motor at a rotation speed of 10 rpm. High purity argon (99.999 %) was supplied as sputtering gas. The flow rate of Ar gas was controlled by mass flow meters (MKS), while the pressure in the chamber was measured by Pirani and Penning gauges. When a base pressure reached to 1.0 $\times 10^{-6}$ mbar, a constant flow of Ar gas was introduced to the chamber at 10 sccm. The RF power and working pressure for sputtering were varied from 50 watts to 200 watts and 0.5×10^{-2} mbar to 2.0×10^{-2} mbar, respectively. During the film fabrications, the GT technique was utilized to fabricate Ag thin films via controlling the on-off sequences of Ar gas at specific temporal intervals in order to operate alternate gas flows into the vacuum chamber as shown in figure 1 (a).[18-25] In this work, the on and off sequences of Ar gas were changed from 10 s to 60 s and 5 s to 15 s, respectively. It should be noted that the deposition processes were carried out at room temperature, i.e. the substrate was not heated during or after deposition. The thickness of Ag thin films was 200 nm, which were measured by thickness monitor (INFICON SQM-160). The fabricated samples were then investigated for the changes in structure and morphology based on the GT technique.

Characterization of silver thin film

The crystal orientation of Ag thin films was examined by X-ray diffractometer (XRD, Bruker D8 ADVANCE). It should be noted that the ratio of (111)/(200) was calculated from the ratio of peak intensity of each crystal plane from XRD. Field emission scanning electron microscope (FESEM, HITACHI SU-8030) and atomic force microscope (AFM, SEIKO SPA400) were employed to investigate the morphology of Ag thin films. The thickness of Ag thin films was measured by using step profiler (MITUTOYO SURFTEST), which was utilized to calibrate an accuracy of thickness monitor.

SERS Measurement

The SERS performance using Ag thin films fabricated via GT rf magnetron sputtering technique was observed. Methylene blue (MB), a Raman active molecule, was employed for testing SERS activity. In this section, the variations in MB concentration of 10^{-6} M to 10^{-13} M (in water) were dropped on the Ag substrates and dried for 15 min in the ambient. A microscopic confocal Raman spectroscopy (NT-MDT NTEGRA SPECTRA) and IX71 Olympus microscope with 100x objective lens, using a laser beam with an excitation wavelength of 532 nm and charge-couple device (CCD) with a resolution of 4 cm^{-1}, was employed to record the SERS spectra. The SERS spectra were acquired with exposure time 10 s and 3 times accumulations. The area of Raman imaging was scanned with 100 μm^2. The exposure time for scan speed and resolution of imaging were 0.3 s per pixel, and 32x32 pixel, respectively

Results and discussion

Figure 1 (b) shows the XRD pattern of Ag thin films grown on Si (111) substrates via using GT rf magnetron sputtering (red line) and conventional sputtering (blue line) techniques, respectively. The thickness of Ag films is 200 nm. Two major diffraction peaks of (111) and (200) of the face-centered-cubic (FCC) Ag structure can be identified on both Ag thin films which correlated to the Joint Committee in Powder Diffraction Standards (JCPDS) file No. 04-0783. It can be seen that a high degree of (111) texture with the (111)/(200) ratio of 40.8 can be obtained via GT technique without applying any additional energy sources, i.e. heating the substrate and/or applying bias on substrate.[18-25] On the other hand, the (111)/(200) ratio of 2.91 can be found in Ag thin film prepared by conventional sputtering. Since the sputtered deposition of Ag thin films actually exhibits a preferred orientation in the (111) direction that is commonly observed in polycrystalline films,[10,13-16] here we examined the peak intensity of (111)/(200) ratio as a function of the on-off gas sequence RF power and working pressure, respectively, for understanding the role of GT technique as shown in figure 2. Figure 2 (a) exhibits the peak intensity of (111)/(200) ratio of Ag thin films as a function of turn-on timing. The turn-off timing is set at 10 s. Below turn-on timing of 50 s, the peak intensity of (111)/(200) ratio increases with increasing turn-on timing. Above turn-on timing of 50 s, the peak intensity of (111)/(200) ratio decreases when turn on timing is increased.

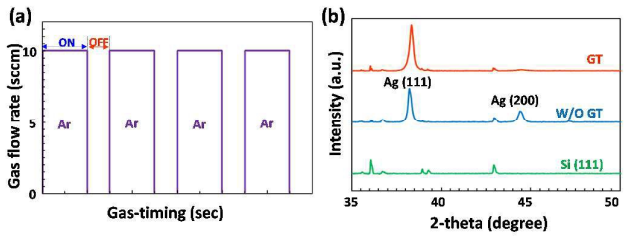

Fig.1 (a) Schematic diagram of gas-timing (GT) rf magnetron sputtering technique (b) XRD patterns of Si (111) substrate (green), Ag thin films grown by conventional sputtering and Ag thin films grown via GT technique (red).

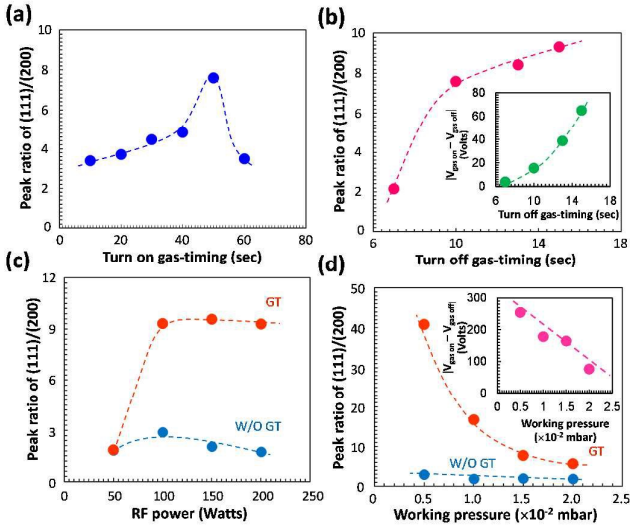

Fig. 2 Peak intensity of (111)/(200) ratio of Ag thin films as a function of (a) turn-on timing and (b) turn-off timing. Inset of fig. 2 (b): Absolute value of the difference in RF bias voltage as a function of turn-off timing (c) Dependence of RF power on (111)/(200) ratio of Ag thin films grown via GT technique (red line) and conventional sputtering (blue line). (d) Dependence of working pressure on (111)/(200) ratio of Ag thin films grown via GT technique (red line) and conventional sputtering (blue line). Inset of fig. 2 (d): Absolute value of the difference in RF bias voltage when varying working pressure. Noted that the on:off sequence of 50 s : 15 s is utilized in fig. 2 (c) and 2 (d).

This enhancement of the crystallinity of Ag thin films with specific turn-on timing value could be frequently observed in the thin films grown via GT technique,[20] which related to a balancing between the GT sequences as to the temporal characteristic of the nucleation and the growth of thin films.[20] The maximum (111)/(200) ratio of 7.60 could be obtained by GT technique at the turn-on timing of 50 s which is higher than that of 2.91 obtained by conventional rf magnetron sputtering. Figure 2 (b) demonstrates the dependence of turn-off timing on the peak intensity of (111)/(200) ratio of Ag thin films. The turn-on timing of 50 s is used. The results show that the (111)/(200) ratio increases when turn-off timing is prolonged. It should be noted that the turn-off sequence could not be longer than 15 s due to the limitation of equipment. Regarding sputtering process, the total energy of sputtered atoms directly correlated with RF power and working pressure, which could be attributed to the transferred energy of Ar^+ to an atom of a target surface, i.e. energy per atom.[10-27] Since an abrupt turn-off sequence could be regarded as the reduction of the working pressure, the higher energy of sputtered atoms could be raised in the longer turn-off sequence. To assure of such explanation, the absolute value of the difference in RF bias voltage between turn-on timing and turn-off timing ($|V_{gas\ on} - V_{gas\ off}|$) is collected during the GT process as shown in the inset of figure 2 (b). It can be seen that the $|V_{gas\ on} - V_{gas\ off}|$ value increases with increasing turn-off timing, implying that the enhancement of energy per atom could be gained at the lower working pressure.[10,11,14,19] Thus the enhancement of the energy per atom through the longer turn-off timing might be responsible for the improvement of (111) orientation texture.[10,11,14,19] Figure 2 (c) shows the dependence of RF power on (111)/(200) ratio of Ag thin films grown via GT technique (red line) and conventional sputtering (blue line). The turn-on: turn-off timing is set at 50 s: 15 s. The peak intensity of (111)/(200) ratio rapidly increases and saturates above RF power of 100 watts when using GT technique, implying that there is a threshold RF power to enhance the (111)/(200) ratio.[11] For the conventional sputtering technique, on the other hand, the (111)/(200) ratio seems to be independent of RF power. Since the energy of sputtered atoms depends on the total energy per number of the sputtered gas, which is directly related to RF power and working pressure, an increasing of the RF power with the constant working pressure does not impact on the total energy in the sputtering system.[10,11,14,19,20] Therefore, the ability to increase the energy of the sputtered atoms can be provided when the GT technique is utilized. In other words, the value of (111)/(200) ratio of Ag thin films can be elevated through the GT technique. Figure 2 (d) demonstrates the dependence of working pressure on (111)/(200) ratio of Ag thin films grown via GT technique (red line) and conventional sputtering (blue line). The RF power and turn-on: turn-off timing of 150 watts and 50:15 are used. It obviously can see that the (111)/(200) ratio strongly depends on the working pressure, especially, when the GT technique is utilized. The maximum value of 40.8 of (111)/(200) ratio can be obtained when the working pressure is at 0.5×10^{-3} mbar. It should be noted that the working pressure could not be operated lower than 0.5×10^{-3} mbar due to the limitation of equipment. On the other hand, the (111)/(200) ratio of Ag thin films grown by the conventional technique slightly increases when the working pressure is decreased. Our results indicate that the effect of working pressure powerfully impacts on the texture orientation of Ag films rather than that of RF power despite without using the GT technique. Recently, Marechal et al. demonstrated that the structure of Ag films sputtered deposited at the low Ar pressure with bias substrate was more oriented in the (111) direction.[11] Since the GT technique can deliver the extra-lower working pressure than the based line of conventional one, the higher kinetic energy during the films growth can be raised when the turn-off sequence is operated. The inset of figure 2 (d) shows the absolute value of the difference in RF bias voltage between turn-on timing and turn-off timing ($|V_{gas\ on} - V_{gas\ off}|$) as a function of the working pressure. It can be seen that the $|V_{gas\ on} - V_{gas\ off}|$ value intensely increase when the working pressure is decreased, implying that the energy of sputtered atoms is powerfully enriched. When the transferred energy increases, therefore, the sputtered atom impinged on the surface of thin films possess the sufficient kinetic energy to enhance the mobility of silver atoms condensed at the film surface.[10,11,13,16] Such adsorbed atoms can move to more preferential favoured site, e.g. void, interstitial position and grain boundary, indicating that an atomic peening phenomenon might be responsible for the improvement of the (111) orientation of Ag thin films.[10-17] To investigate the effect of atomic peening on Ag film texture, here we have observed the cross-section and morphology of Ag thin films grown via GT technique and conventional sputtering as shown in figure 3 (a-b). The cross-section and the morphology of Ag films are observed by using FE-SEM and AFM, respectively. It should be

noted that the thickness of 1 µm of Ag thin films is prepared to compare the distinct difference between the texture of Ag thin films grown via GT technique and conventional sputtering. The results demonstrate that the Ag thin film grown via the GT technique exhibits a finer columnar structure than that via the conventional sputtering.[10] This implies that the Ag films deposited via the GT technique should be submitted to a relatively intense bombardment of high-energy particles during the turn-off sequence and then the silver atoms condensed on the film surface can move to the deeper positions in the film texture. Consequently, a fully dense structure of Ag films can be obtained.[26] The insets of figure 3 (a) and 3 (b) demonstrate the morphology of Ag films. It can be seen obviously that the GT technique produces a smaller grain size (~80 nm) than that of the conventional sputtering (~200 nm). Therefore, the atomic peening effect emerged from the GT technique is responsible for the fine columnar of Ag film texture due to the ability to enhance energetic mobile atoms on the film surface. Such fine columnar structure resulting from the mobility of adatoms as a function of (111)/(200) ratio can improve the conductivity of Ag thin films as shown in supporting information 1†.[10,11] Figure 3 (c) shows the grain size and RMS roughness of Ag thin films as a function of (111)/(200) ratio. The peak intensity of (111)/(200) ratio inversely correlates to the grain size and roughness RMS of Ag films, indicating that the capability to adjust the peak intensity of (111)/(200) ratio directly affects on the morphology of Ag thin films. Here we question what is the possible mechanism that the GT technique enables us to induce the texture orientation of (111) Ag thin films. Within the frameworks of the sputtering technique, Ar^+ ions are generated via RF excitation or high voltage between anode and cathode.

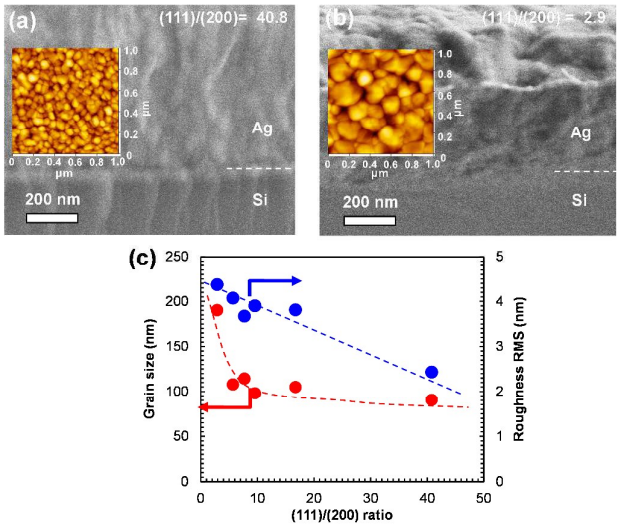

Fig. 3 Cross-section images of Ag thin films grown via (a) GT technique and (b) Conventional sputtering. Inset of fig. 3 (a) and 3 (b) shows AFM images. 3 (c) Grain size and RMS roughness of Ag thin films grown via GT technique as a function of (111)/(200) ratio.

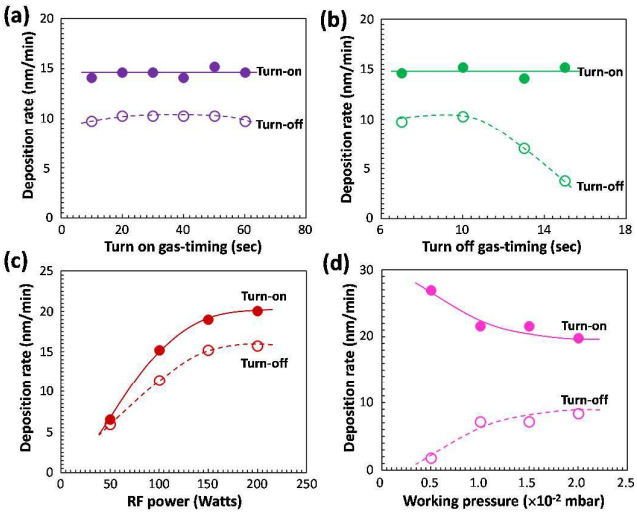

Fig. 4 The deposition rate of Ag thin films grown via GT technique during growth as a function of (a) turn-on gas-timing, (b) turn-off gas-timing, (c) RF power and (d) working pressure. Full circle is the deposition rate of turn-on timing whereas blank circle is the deposition rate of turn-off timing.

When Ar^+ ions bombard on the target materials, the energy and momentum transferred to atoms at the surface of target can knock some of these atoms off the target surface. Subsequently, such sputtered atoms will travel to a substrate and deposit as a thin film with high kinetic energy. Since the deposition rate of sputtering related to energy and momentum transfer (energy per atom) is proportional to the sputtering yield, which straightforwardly depends on working pressure and RF bias voltage, the ability to optimize the kinetic energy during sputtering process is very important to adjust the sufficient energy for texture orientation.[26] Figure 4 (a)-(d) exhibit the deposition rate of Ag thin films grown via the GT technique as a function of (a) turn-on gas-timing, (b) turn-off gas-timing, (c) RF power and (d) working pressure. Noted that full circle is the growth rate of turn-on gas and blank circle is the growth rate of turn-off gas. It can be clearly seen that the deposition rate of turn-on gas is almost higher than that of turn-off gas. Since the turn-off gas sequence can be attributed, as the reduction of the working pressure, the decrease of the deposition rate as to the lower amount of sputtered atoms will raise the energy per atom of particles. Such energetic particles will transfer energy and momentum to Ag atoms condensed on the film surface, resulting that the mobility of adatoms can be occurred as followed the atomic peening effect.[26,27] On the other hand, the deposition rate of the turn-on gas sequence can be considered same as the growth rate of thin films prepared by the conventional sputtering deposition. Since the total kinetic energy of the system related to $|V_{gas\ on} - V_{gas\ off}|$ can be elevated by utilizing GT technique as shown in figure 2 (a-d), the difference in the deposition rate between turn-on and turn-off gas (ΔR) may allow us to determine the

enhancement of the texture formation (i.e. the large difference of ΔR effectively enhances crystal orientation, Supporting information 2)†. Although the ΔR seems to be constant in figure 4 (a) when varying the turn-on gas sequence, the ΔR increases when the turn-off gas sequence is prolonged as shown in 4 (b). Furthermore, we found that the ΔR is strongly dominated by working pressure rather than that of RF power, which is corresponding to the increase of $|V_{gas\ on} - V_{gas\ off}|$ in figure 2 (c) and 2 (d). Therefore, the alternate GT sequence during the deposition might be the switching mode between deposition mode and self-energy assisted mode, which generate the atomic peening mechanism through high kinetic energy (Supporting information 3). Thus, our results highlight that employing the GT technique enables us to control and design the texture engineering of sputtered face-centered-cubic (FCC) metal thin films (e.g. Ag, Au, Cu and Al) without applying any additional energy sources such as heating and RF bias at substrate during growth.

Finally, we demonstrate the utilizing of Ag thin films grown via GT technique as a SERS substrate as shown in figure 5 (a-d). The thickness of Ag thin films is fixed at 200 nm. Figure 5 (a) demonstrates the Raman spectra of MB at the concentration of 1×10^{-13} M on Ag thin films grown by GT technique (green line), Ag thin films grown via conventional sputtering (blue line) and blank substrate (Si, red line). The peak at 520 cm^{-1} corresponds to the Raman scattering of the crystalline Si substrate. It can be seen that the Raman signal of MB with the concentration of 10^{-13} M can be observed only when the Ag thin film grown via GT technique is utilized. This indicates that the GT technique enables us to fabricate high sensitivity of SERS substrate. Figure 5 (b) exhibits the dependence of MB concentration on SERS intensity. Noted that the SERS intensity of MB is collected from the characteristic of Raman shift at 1626 cm^{-1}. It can be seen that although the SERS intensity of Ag thin film grown via GT technique rapidly decreases when the concentration of MB decreases from 10^{-6} M to 10^{-8} M, the Raman spectra of MB can be found at the MB concentration of 10^{-13} M (figure 5 (a)). On the other hand, the SERS intensity of Ag thin film prepared by conventional sputtering cannot be detected below the MB concentration of 10^{-7} M. For more information, we have determined the enhance factor (EF) to compare the SERS enhancement between Ag thin film grown via GT technique and conventional sputtering. Here the EF is defined as a ratio of elastic scattering intensity per molecule between the presence and absence of SERS.[6,7,28-36] The Raman EF is written as $EF = \frac{I_{SERS}}{I_{Ref}} \cdot \frac{N_{Ref}}{N_{SERS}}$, when I_{SERS} is the enhance intensity of adsorbed MB molecules on the SERS substrate. I_{Ref} is the spontaneous Raman scattering intensity from the bulk MB molecules under the laser spot on the blank Si substrate. N_{Ref} is defined as the number of the bulk MB molecules excited by the laser without Raman enhance effect.

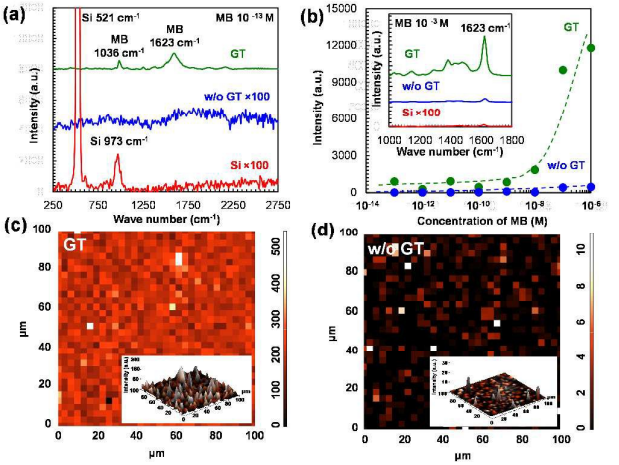

Fig. 5 (a) Raman spectra of methylene blue (MB) droplets at concentration of 10^{-13} M dried on Si (red), Ag thin films grown via conventional sputtering (blue) and Ag thin films grown via GT technique (green). (b) SERS intensity collected at Raman shift of 1626 cm^{-1} of Ag thin films prepared by conventional sputtering (blue) and GT technique (green). Inset of figure 5 (b) shows Raman spectra of MB droplets at concentration of 10-3 M dried on Si (red), Ag thin films grown via conventional sputtering (blue) and Ag thin films grown via GT technique (green). (c) Raman spectra mapping of SERS substrate fabricated via GT technique and conventional sputtering, respectively. Insets of figure 5 (c) and 5 (d) show the Raman mapping of SERS substrates prepared by GT technique and conventional sputtering. Noted that the Raman signal peak of 1626 cm^{-1} of MB is set to scan for SERS mapping. The MB concentration of 10^{-6} M is used to observe.

For MB concentration of $1.0\text{x}10^{-3}$ M, N_{Ref} is approximately $1.7\text{x}10^{8}$ molecules within a scattering volume of 1000 μm^3.[6,28,30] N_{SERS} is the number of MB molecules uniformly spreading on the SERS substrate under the laser spot. Using a 100x objective lens, the area of the laser spot is around 1 μm^2. Assuming a monolayer of the adsorbed molecules, the value of N_{SERS} under laser excitation is therefore $5\text{x}10^{5}$ molecules.[6,28,30] By collecting the intensity of characteristic of Raman shift at 1626 cm^{-1} of Ag thin film grown via GT technique, Ag thin film grown via conventional sputtering and blank from the inset of figure 5 (b), we can obtain the average values of EF of Ag thin films grown via GT technique and conventional sputtering as $3.40\text{x}10^{5}$ and $1.42\text{x}10^{4}$, respectively. This result indicates that the EF of Ag thin film grown via GT technique is higher than that of Ag thin film grown via conventional sputtering 1 order. Since the performance enhancement of sputtered SERS substrate can be explained through the hot spots effect[5-8,28-36] which directly depends on the morphology of thin films,[5-8] here we have collected the RMS roughness, grain size, gap between grain edges and density of grain of Ag thin films by AFM as shown in table 1. The results demonstrate that the RMS roughness, grain size and gap between grain edges of the Ag thin films grown via the GT technique are smaller than that of the Ag thin films grown via the conventional sputtering. On the other hand, the density of grain size of Ag thin films grown via the GT technique is higher than that of the Ag thin films grown via the conventional sputtering. Although the RMS roughness of the Ag thin film prepared by the conventional

sputtering is smaller than that of the GT technique, Lee et al. recently demonstrated that the roughness of sputtered Ag films with the thickness higher than 20 nm could not enhance SERS activity due to limited effect of SERS process.[9] Therefore the effect of roughness with the thickness of 200 nm can be eliminated.[5,9] For the grain size effect, as the particle size increases, the particles absorb less light and scatter more through inelastic scattering, which should decrease the overall SERS intensity.[5,9,28,31-34] Furthermore, the increase in the grain size with the lower density of grain leads to the reduction of the total surface area for adsorption.[5,33,34] Since the large EM field enhancement is located at the junction between individual particles, the EM enhancement in these spatially confined hot spots can be larger orders of magnitude than on the individual particle surface.[5-9,28-36] Yan et al.[31] and McMahon et al.[33] showed that the smaller gap between particles give a higher SERS enhancement. This indicates that the smaller gap between grain edges fabricated by the GT technique should be included in the factors that increase SERS enhancement. Figure 5 (c) and 5 (d) exhibit SERS mapping of Ag thin films grown via the GT technique and the conventional sputtering. Noted that the scan speed of 0.3 s/pixel is used. The Raman signal peak of 1626 cm^{-1} of MB is set to scan for SERS mapping. The MB concentration of 10^{-6} M is used to observe. It can be obviously seen that the uniformity of SERS signals can be accomplished when the SERS substrate fabricated by the GT technique is utilized. Whereas SERS signals from using the conventional sputtered SERS substrate shows low non-uniform distribution of SERS signals, implying that Ag thin films prepared by GT technique are promising for SERS activities. Noted that the further investigation is in progress. Thus, our results highlight that controlling and designing the texture orientation of Ag thin films through the GT technique enable us to fabricate the high performance SERS substrate.

Conclusions

In this work, we have demonstrated the special technique so called gas-timing (GT) rf magnetron sputtering which allow us to control a texture orientation of Ag thin films without applying any additional energy sources (i.e. pre/post annealing and/or bias substrate). We found that the GT technique as to the on-off sequence switching can be attributed to the alternate sequence between deposition mode and energy-assisted mode during thin film growth. Such switching modes through the GT technique not only provide the ability to adjust the number of sputter species from the target but also generate self-energy assisted, which related to the atomic peening effect. In addition, we exhibit that the high (111)/(200) ratio of Ag films strongly affects on the SERS activity of Ag films due to the small grain size and the gap between grain edges (i.e. hot spot effect). Our results highlight that utilizing the GT technique enables us to perform the texture engineering of metal thin films which can apply for various research fields.

Table 1. RMS roughness, grain size, gap between grain edges and density of grain of Ag thin films.

Ag thin films SERS substrate	RMS Roughness (nm)	Grain size (nm)	Gab between grain edge (nm)	Density of grain (grain/μm^2)
GT technique	2.4	80.3	55.2	306
Conventional sputtering	4.4	190.5	85.6	90

Acknowledgements

This work was partially supported by Research and Development of White Light Emitting Diode based on Zinc Oxide Optoelectronics Material; Phase-1: Method of ZnO-Substrate Fabrication project (P1450015) from the National Science and Technology Development Agency, Thailand.

References

1 G. Grolig and K-H Kochem, Adv. Mater., 1992, 4, 179-188
2 C. Dellacorte, H. E. Sliney and D. L. Deadmore, Tribol. Trans., 1988, 31, 328-333.
3 C.Dellacorte, S. V. Peper and F. S. Honecy, Surf. Coat. Technol., 1992, 52, 31-37
4 Y. Zeng, T. L. Alford, Y. L. Zou, A. Amali, B. M. Ullrich, F. Deng and S. S. Lau, J. Appl. Phys., 1998, 83, 779-785
5 D. J. Semin, and K. L. Rowlen, Anal. Chem., 1994, 66, 4324-4331
6 N. Nuntawong, M. Horprathum, P. Eiamchai, K. Wong-ek, V. Patthanasettakul, P. Chindaudom, Vacuum, 2010, 84, 1415-1418
7 J. Perumal, K. V. Kong, U. S. Dinish, R. M. Bakker and M. Olivo, RSC Adv., 2014, 4, 12995-13000
8 G. Santoro, S. Yu, M. Schwartzkopf, P. Zhang, S. K. Vayalil, J. F. H. Risch, M. A. Rubhausen, M. Hernandez, C. Domingo and S. V. Roth, Appl. Phys. Lett., 2014, 104, DOI: 10.1063/1.4884423
9 C. Lee, C. S. Robertson, A. H. Nquyen, M. Kahraman and S. Wachsmann-Hogiu, Sci. Rep., 2015, 5:11644, DOI: 10.1038/srep11644
10 N. Marechal, E. Quesnel, and Y. Pauleau, J. Vac. Sci. Technol. A, 1994, 12, 707-713
11 N. Marechal, E. Quesnel and Y. Pauleau, Thin Solid Films, 1994, 241, 34-38
12 Y. Zeng, Y. L. Zou, T. L. Alford, F. Deng, S. S. Lau, T. Laursen and B. M. Ullrich, J. Appl. Phys., 1997, 81, 7773-7777
13 L. Dong and D. J. Srolovitz, J. Appl. Phys., 1998, 84, 5261-5269
14 K.-F. Chiu and Z. H. Barber, Thin Solid Films, 2000, 358, 264-269
15 A. Rizzo, M. A. Tagliente, M. Alvisi and S. Scaglione, Thin Solid Films, 2001, 396, 29-35
16 V. Kapaklis, P. Poulopoulos, V. Karoutsos, Th.Manouras and C. Politis, Thin Solid Films, 2006, 510, 138-142
17 J. Lv, F. Lai, L. Lin, Y. Lin, Z. Huang and R. Chen, Appl. Surf. Sci., 2007, 253, 7036-7040
18 N. Kietipaisalsophon, W.Bunjongpru, W. Techitdheera and J. Nukeaw, 2002 IEEE International Conference on Industrial Technology : Productivity reincarnation through robotics & automation, IEEE, Asian Institute of Technology, 2002, 02, 1365-1367

19 A.Klamchuen, N. Pornteeraphat and J. Nukeaw, e-J. Surf. Nanotech., 2005, 3, 272-275
20 D. Klaitabtim, S. Pratontep and J. Nukeaw, Ceram. Inter., 2008, 34, 1103-1107
21 D. Klaitabtim, S. Pratontep and J. Nukeaw, Jpn. J. Appl. Phys., 2008, 47, 653-656
22 A. Sungthong, S. Porntheeraphat, A. Poyai and J. Nukeaw, Appl. Surf. Sci., 2008, 254, 7950-7954
23 S. Porntheeraphat and J. Nukeaw, Appl. Surf. Sci., 2008, 254, 7851-7854
24 A. Poyai, W. Bunjongpru, N. Klunngien, S. Porntheeraphat, C. Hruanan, S.Sopitpan and J. Nukeaw, Mat. Sci. Semi. Proc., 2008, 11, 319-323
25 W. Techitdheera, C. Thassana, W. Pecharapa, and J. Nukaew, 2010 3rd International Nanoelectronics Conference: (INEC 2010), IEEE, City University of Hong Kong, 2010, 03, 1151-1152
26 K.-H. Muller, Phys. Rev. B, 1987, 35, 7906-7913
27 A. J. Detor, A. M. Hodge, E. Chason, Y. Wang, H. Xu, M. Conyers, A. Nikroo, A. Hamza, Acta Mater., 2009, 57, 2055-2065
28 G. Laurent, N. Felidj, J. Aubard, G. Levi, J.R. Krenn, A. Hohenau, G. Schider, A. Leitner and F.R. Aussenegg, Phys. Rev. B, 2005, 71, 045430
29 M. Moskovits, J. Raman Spectrosc., 2005, 36, 485-496
30 G.-N. Xiao and S.-Qing Man, Chem. Phys. Lett., 2007, 447, 305-309
31 B. Yan, A. Thubagere, W. R. Premasiri, L. D. Ziegler, L. D. Negro and B. M. Reinhard, ACS Nano, 2009, 3, 1190-1202
32 K. G. Stamplecoskie and J. C. Scaiano, J. Phys. Chem. C, 2011, 115, 1403-1409
33 J. M. McMahon, S. Li, L. K. Ausman and G. C. Schatz, J. Phys. Chem. C, 2012, 116, 1627-1637
34 Z. Huang, G. Meng, Q. Huang, B. Chen, C. Zhu, and Z. Zhang, J. Raman Spectrosc., 2013, 44, 240-246
35 A. Saha, S. Palmal and N. R. Jana, Nanoscale, 2012, 4, 6649
36 T. Yang, E. Wang, F. Wang, K. Chou and X. Hou, Sci. Rep., 2015, 5:9690, DOI: 10.1038/srep09690